Reservoir evaluation of Upper Permian buildups in the Jameson Land basin, East Greenland

Lars Stemmerik

GRØNLANDS GEOLOGISKE UNDERSØGELSE
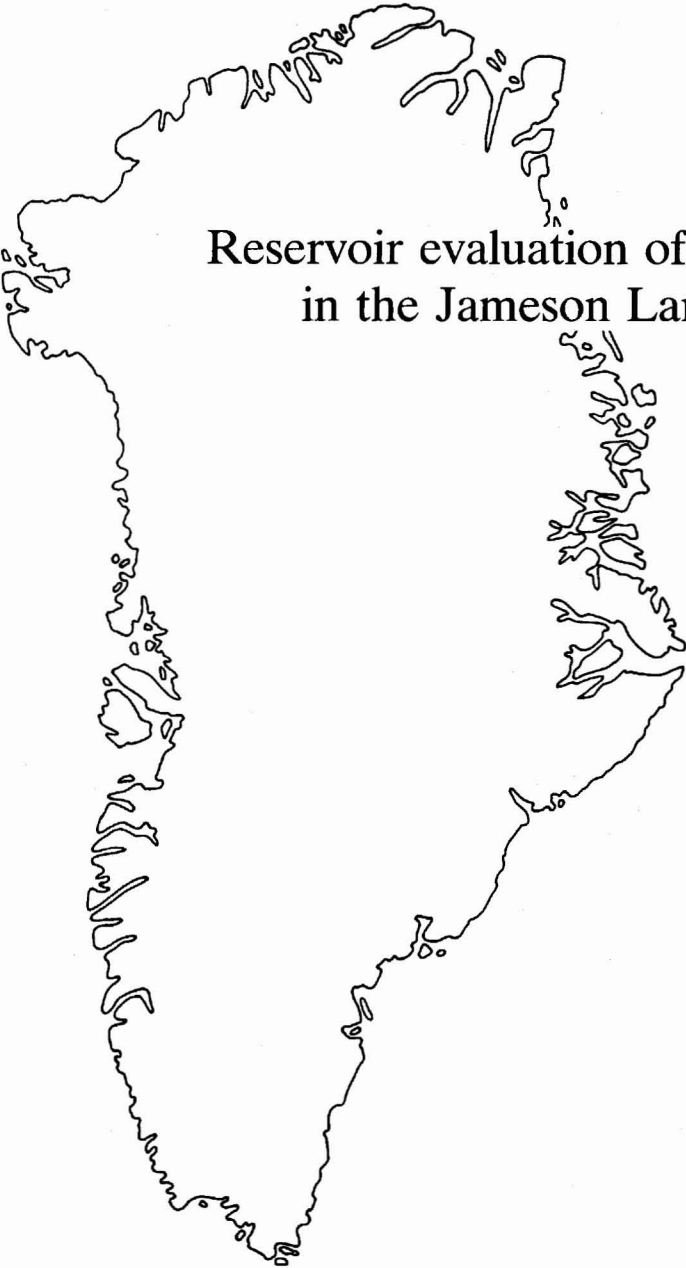
GGU

Rapport 149

1991

Reservoir evaluation of Upper Permian buildups in the Jameson Land basin, East Greenland

Lars Stemmerik

1991

Dansk sammendrag

Bryozorev af sen Perm alder menes at være en af de vigtigste reservoirenheder for kulbrinter i Jameson Land bassinet i det centrale Østgrønland.

Denne rapport vurderer reservoiregenskaberne af disse rev på basis af studier af overflademateriale fra østranden af bassinet. Revene blev cementeret allerede mens de stod på havbunden, og deres oprindelige porøsitet var tæt på 0%. Senere er en del aragonit blevet opløst som følge af ferskvandsgennemstrømning, og på det tidspunkt, da der migrerede kulbrinter ind i revene, havde de ca. 10% porøsitet. Revene blev sandsynligvis fyldt med kulbrinter i sen Kridt, men for ca. 20 millioner år siden blev de gennemstrømmet af varmt vand, olien blev presset ud og porerne fyldt med kalcit cement, baryt, fluorit og galena.

Den sene, hydrotermale begivenhed er formentlig relateret til hævningen af undersøgelsesområdet på Wegener Halvø og menes derfor ikke at have påvirket revene i selve Jameson Land bassinet.

Imaqarnersiuineq

Ikkanneq isorartooq Bryozorev, Perm-ip naalernerani, tassa ukiut 250 milliunit matuma siornatigut pinngorsimasoq, Tunumi Jameson Landip imartunerisimasaani nunami qaleriiaat immikkoortuisa uuliamik katersuuffiusinnaasut pingaarnersaattut naatsorsuuneqarpoq.

Nalunaarusiaq una imartunerusimasup kangiatungaani nunap qaavata sananeqaataanik misissuinerit tunngavigalugit uuliap ikkannerni taakkunani katersuuffigisinnaassusianik naliliisuuvoq. Ikkannerit immap naqqaniitillutik tiggussorsimapput, taamaammallu aallaqqaammut ussissorujussuusimallutik. Kingorna imermik tarajoqanngitsumik aqqusaarneqarnertik pissutigalugu, sioqqat sananeqaataasa ilaat, aragonit, aassima-voq. Uuliallu ikkannernut isaanerata nalaani kisitsisinngorlugu 10% missaani ussiissuseqarsimallutik. Ikkannerit Kridt-ip naalernerani, tassa ukiut 70 milliunit matuma siornatigut, uuliamik akoqalersimapput, ukiulli 20 milliunit matuma siornatigut imermik kissartumik aqqusaarneqarsimallutik. Taamaalillunilu uulia suppugussaasimavoq, putuaraararpassuillu uuliamik imaqarsimasut qeqormik, baryt-imik, flourit-imik aqerlussamillu taarserneqarlutik.

Taamak kingusinnerusukkut imermik kissartumik aqqusaarneqarsimanerat Wegener Halvø-imi misissuiffiusup qaffanneranut atassuteqarsimagunarpoq, taamaattumillu Jameson Land-ip imartunerisimasaani.

Reservoir evaluation of Upper Permian buildups in the Jameson Land basin, East Greenland

Lars Stemmerik

The Upper Permian Wegener Halvø Formation buildups form an important reservoir target in the Jameson Land basin. Due to absence of subsurface information from the basin, reservoir properties of the buildups are tentatively evaluated by timing the different diagenetic modifications seen in outcrop relative to hydrocarbon migration. The buildups became cemented during deposition and the ultimate porosity was close to zero. Post-depositional porosity appears to be related to freshwater dissolution of aragonite cement during Permian exposure events.

Reservoir potential is mainly confined to the buildup cores and the proximal flank deposits. Porosity prior to hydrocarbon migration is estimated to average 10% in the buildups and 5–6% in the proximal flank deposits. Pores became filled by hydrocarbons probably in the Late Cretaceous; the reservoirs became flushed by hot, hydrothermal fluids c. 20 Ma ago and pores are now filled by iron-rich calcite, baryte and fluorite. The flushing of the reservoir may be related to the Tertiary uplift of Wegener Halvø, and it is most likely a local event not affecting the basin as a whole.

L. S., Geological Survey of Greenland, Øster Voldgade 10, DK-1350 Copenhagen K, Denmark.

This paper describes the results of a research programme initiated by the Geological Survey of Greenland (GGU), and economically supported by the Mineral Resources Administration for Greenland, Ministry of Energy, to evaluate the reservoir potential of the carbonate buildups in the Upper Permian Wegener Halvø Formation of Jameson Land, East Greenland on the basis of surface data. Buildups of the Wegener Halvø Formation formed an important reservoir target in the exploration of the Jameson Land basin that until recently was undertaken by a group comprising ARCO International and AGIP. However, after this paper was submitted, the ARCO group announced its decision not to proceed to a drilling phase and in consequence they relinquish their concession at the end of 1990. This study therefore rather provides a background for assessing the reservoir potential of the Upper Permian carbonates during any future exploration in the basin. Buildups are exposed along the basin margins with the best examples found in outcrops in Wegener Halvø along the eastern margin (Fig. 1) (Surlyk et al., 1986; Hurst et al., 1989; Stemmerik et al., 1989).

The critical issue in evaluating reservoir properties of carbonate rocks from outcrop samples is the timing of diagenetic modifications relative to hydrocarbon generation and migration. In Wegener Halvø, unlike most other areas along the basin margin, Upper Permian sediments have been buried to depths where hydrocarbon generation and migration took place (Surlyk et al., 1986; Christiansen et al., 1990), and migrated hydrocarbons have been discovered in several of the buildups in the area (Hurst et al., 1989; Stemmerik et al., 1989). The detailed relationship between the different types of carbonate cement and the migrated hydrocarbons can therefore be studied directly in this area. Wegener Halvø was chosen as the main study area for this research programme which included a joint ARCO, AGIP and GGU field programme focusing on the overall depositional history of the Wegener Halvø Formation (Stemmerik et al., 1989), and a GGU shallow drill programme (Christiansen & Stemmerik, 1989). The aim of the drill programme was to obtain representative material from the central, inaccessible parts of the buildups, in order to better understand their depositional history.

This paper focuses on evaluating the reservoir potential of the Wegener Halvø Formation buildups on the basis of two shallow cores from two nearby buildups south of Paradigmabjerg (Fig. 2). Also included in this study is a shallow core drilled through the proximal flank deposits of a buildup in Devondal (Fig. 2); in total more than 180 m of core have been investigated. While
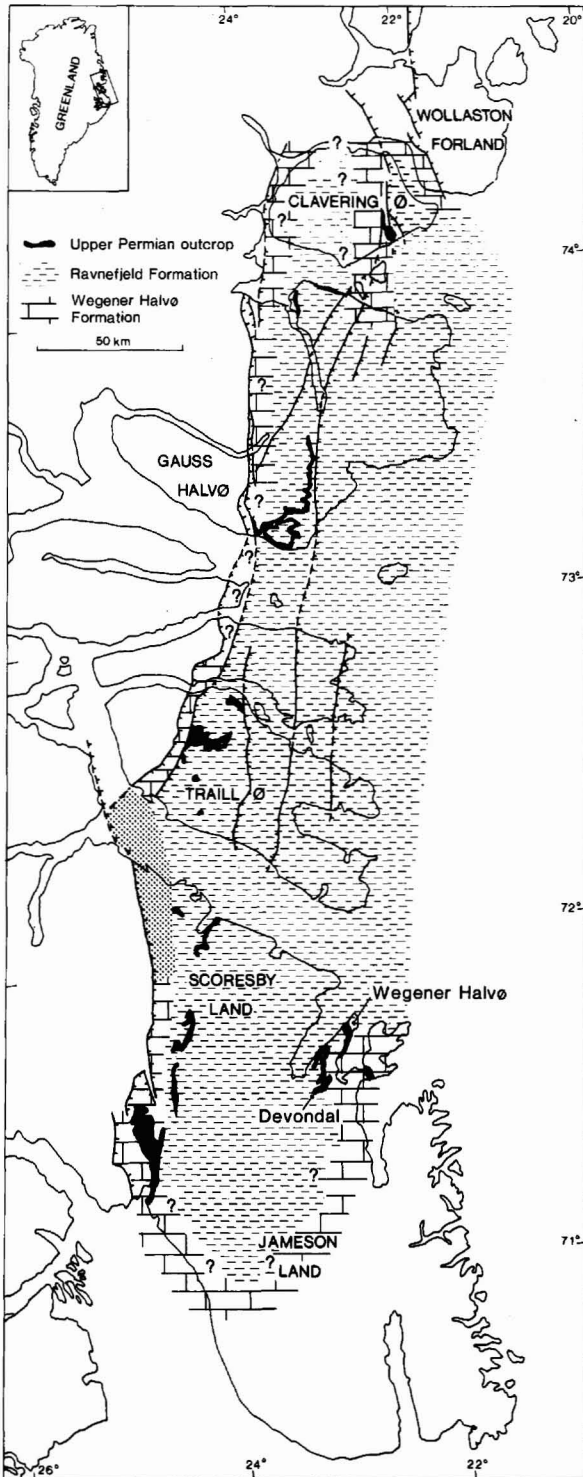
Fig. 1. Map showing the outcrops of Upper Permian sediments in central East Greenland and the suggested outline of the depositional basin.
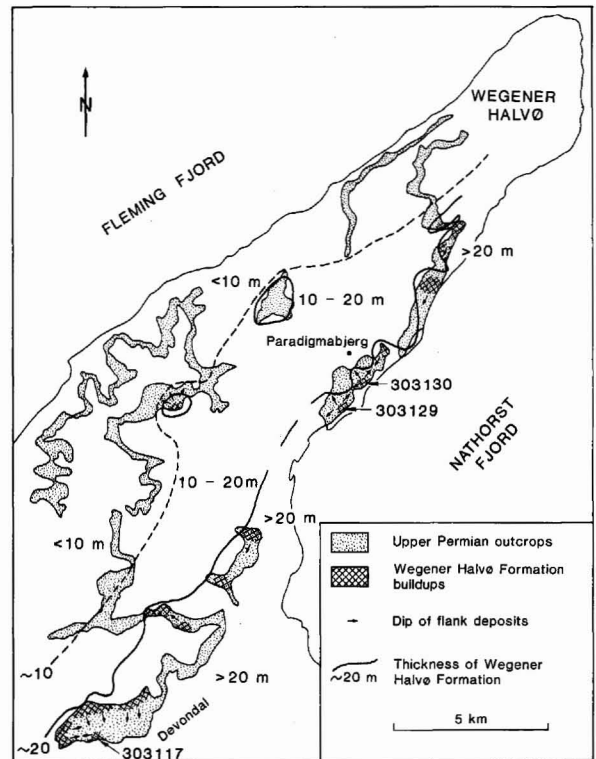

Fig. 2. Detailed map of Wegener Halvø showing present-day outcrop, thickness of the Wegener Halvø Formation, location of buildups and location of investigated cores.

this paper concentrates on the reservoir potential of the buildups and the implications for the Jameson Land basin as a whole, the more detailed diagenetic investigations which form the basis for this study and contributions of more regional significance will be reported elsewhere (Scholle *et al.*, in press; Stemmerik *et al.*, in press).

Regional setting

The Wegener Halvø area is situated along the southeastern margin of the Late Permian depositional basin in central East Greenland (Fig. 1) (Maync, 1961). The area formed a structural high during Carboniferous and Early Permian times, so that folded Devonian strata are unconformably overlain by Upper Permian sediments (Fig. 3).

The Upper Permian depositional sequence diplays several major transgressive-regressive cycles; the oldest sediments are fluviatile to fluviomarine conglomerates. The first marine transgression into the region since the Early Palaeozoic is recorded by widespread deposition of shallow water, restricted marine limestones and mi-
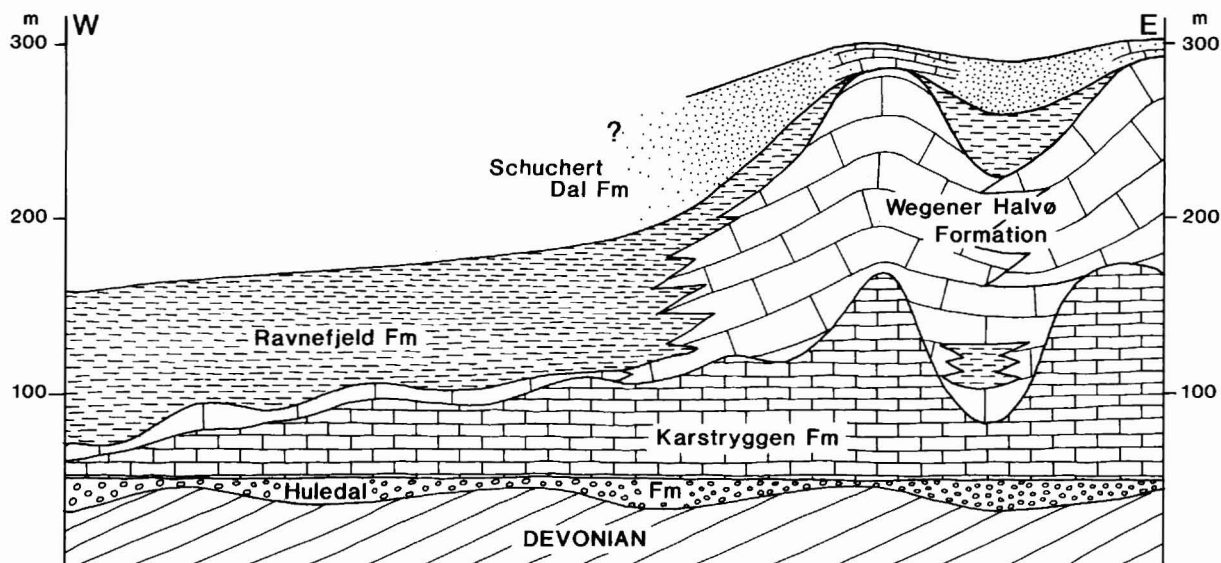
Fig. 3. Schematic E–W cross-section illustrating the distribution of the principal lithostratigraphic units throughout Wegener Halvø.

nor evaporites of the Karstryggen Formation (Fig. 3) (Surlyk *et al.*, 1986). A major fall in sea-level terminated deposition and the Karstryggen Formation sediments were subjected to erosion, resulting in a mature fluvially induced palaeo-karst terrain with as much as 70 m of relief along the eastern basin margin. This erosional event was apparently accompanied by westward tilting of the Wegener Halvø high; the combined result was a highly irregular surface to the east and a topographically lower, smoother surface to the west.

A second major transgression later in the Permian led to renewed flooding of the area. The depositional pattern became more differentiated during this event, mainly as a consequence of the highly irregular topography developed on top of the Karstryggen Formation. Carbonate buildups within the Wegener Halvø Formation are located above palaeotopographic highs to the east, while the western lowland soon was drowned and became the site of deeper water shale deposition (Fig. 3) (Stemmerik *et al.*, 1989).

The buildups investigated in this study are located on palaeotopographic highs towards the east (Fig. 2). The buildups south of Paradigmabjerg are situated on two highs separated by an east–west trending palaeo-valley. The foundation below the Devondal buildup is not known in detail, but apparently this buildup is also situated on an isolated high. The more closely spaced buildups merged to form a semi-continuous carbonate platform during late Wegener Halvø Formation times. The youngest carbonates in this platform area are oolitic and shallow water biogenic grainstones, suggesting

that the carbonate platform gradually became more shallow and finally was exposed.

Late Permian sedimentation was terminated by deposition of a sequence of siliciclastics belong to the Schuchert Dal Formation. Sedimentation during this final Permian pulse was controlled, along the basin margins, by the topography of the underlying carbonates (Fig. 3).

Sedimentology

The investigated cores were drilled through different parts of the buildups and therefore display a variety of sedimentary facies and diagenetic modifications.

Core GGU 303129 is from near the crest of a buildup south of Paradigmabjerg (Figs 2, 4). The core was drilled through an upper sequence of grainstones and packstones down into the main buildup. Core GGU 303130, located on the adjacent buildup some 500 m to the north (Figs 2, 4, 5), starts in the main buildup and continues down into the underlying Karstryggen Formation. Core GGU 303117 is from the western side of a major buildup in Devondal (Figs 2, 6). This core was drilled through a sequence of flank deposits and small bryozoan mounds prograding down the flank of the main buildup (Fig. 6) (Hurst *et al.*, 1989). This core has not been studied in any great detail, but has been included to enable an evaluation of the porosity development of the flank deposits.

The cored material is believed to be representative of the sedimentary and diagenetic fabrics in the main build-
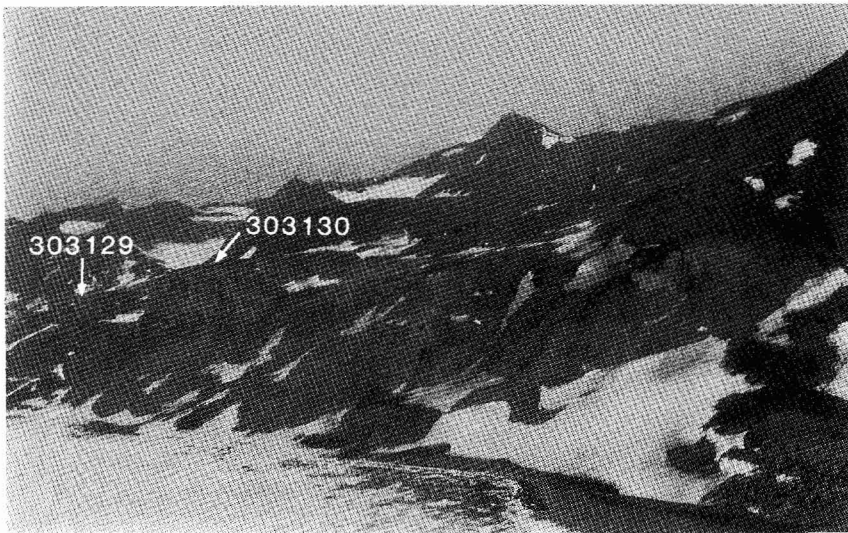
6

Fig. 4. East coast of Wegener Halvø seen from the north-east. Arrows point to location of cores GGU 303129 and 303130.
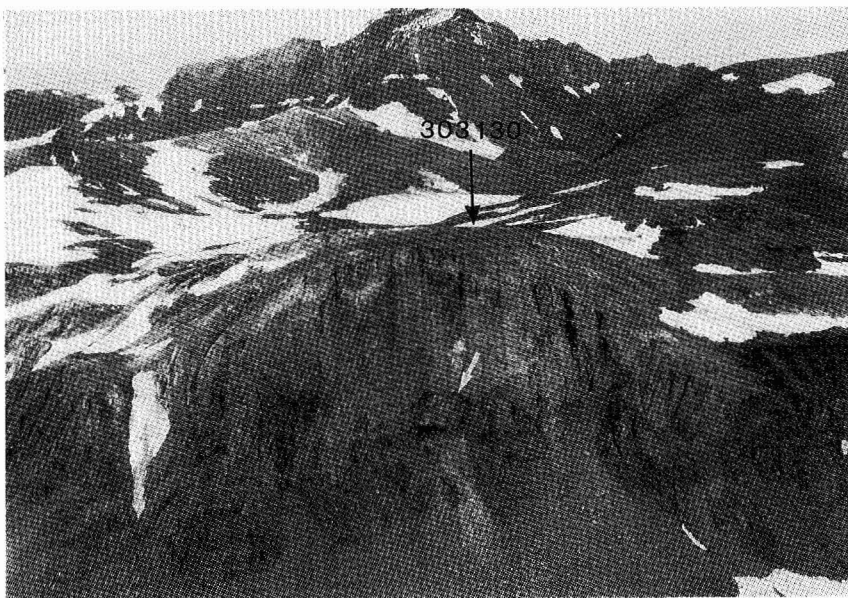

Fig. 5. The buildup encountered by core GGU 303130 showing massive core facies surrounded of bedded flank deposits. Arrow points to the surface of the Karstryggen Formation.
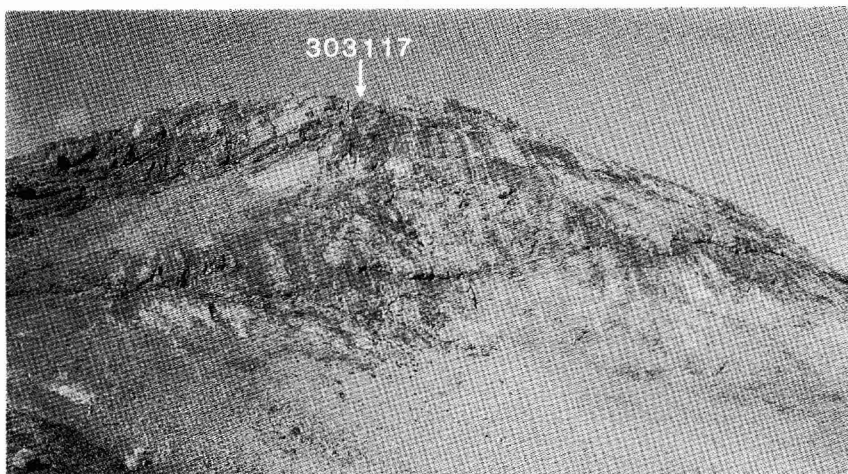

Fig. 6. Southern margin of the Devondal buildup showing small bryozoan mounds prograding down the slope of the main buildup. Location of core GGU 303117 shown by arrow.

ups and the proximal parts of the flank deposits. Porosity evaluations of the more distally deposited flank deposits are based on previous studies (Surlyk *et al.*, 1986; Hurst *et al.*, 1989; Scholle *et al.*, in press), supplemented by semi-quantitive estimates based on core GGU 303117. The following brief description of the buildups focuses mainly on the rock characteristics; a more detailed description of the buildups and their depositional history will be given by Stemmerik *et al.* (unpublished manuscript).

Buildup frame

The main buildups, as represented by cores GGU 303130 (0–80.6 m) and GGU 303129 (34.0–53.0 m), are dominated by shallow water facies with large amounts of early marine cement (Figs 7, 8). Three distinctly different facies are distinguished in this study.

Bivalve-oncolite grainstone. This facies is dominated by thin-shelled bivalves and/or oncolites (Figs 9, 10). The bivalves are commonly encrusted by tubular foraminifers or more rarely by encrusting bryozoans. The diversity of the fauna is extremely low; the bivalves form monospecific assemblages and other faunal elements are apparently represented by only one species each.

Bivalve shells and oncolites have been leached and the resulting pores subsequently filled by equant, iron-poor calcite crystals (Figs 10, 11). The pore space between grains is partly filled by early marine cements; remaining pore space is filled mainly by equant, iron-poor calcite crystals similar to those replacing the grains.

This facies represents deposition in shallow marine, high to moderately high energy environments. The impoverished fauna implies deposition under biologically stressed, most likely hypersaline conditions. A similar facies was found in (possibly tidal) channels between stromatolite heads near the base of a buildup further to the west (Stemmerik *et al.*, 1989).

Although the replacement of the original aragonitic shell material with calcite is taken as an indication for fresh water flushing of the sediment, there is no indication of prolonged subaerial exposure during deposition, and this freshwater event is believed rather to be related to later (?Permian) exposure of the entire mound.

Marine cementstone. This facies includes a variety of sediments where the dominant constituent is early marine cement (Figs 12, 13, 14). Commonly, more than 80% of the bulk volume consists of early marine cements. Other important constituents are algae and biv-

Fig. 7. Sedimentary log of core GGU 303129 with variations in estimated palaeo-porosity.

Legend:

Symbol	Description
Non-bedded limestone	
Thin bedded limestone	
M	Mudstone
W	Wackestone
P	Packstone
G	Grainstone
C	Cementstone
B	Boundstone
✹	Encrusting bryozoan
Y	Non-encrusting bryozoan
℘	Tubular foraminifer
℘	Foraminifer, unspecified
<	Bivalve
⌣	Brachiopod
&ᵣ	Algae
▽	Marine cement
◇	Intraclast

alves, and occasionally the rock is better termed a boundstone.

The early marine cement occurs as radiating botryoids of cloudy and peloidal iron-poor calcite with
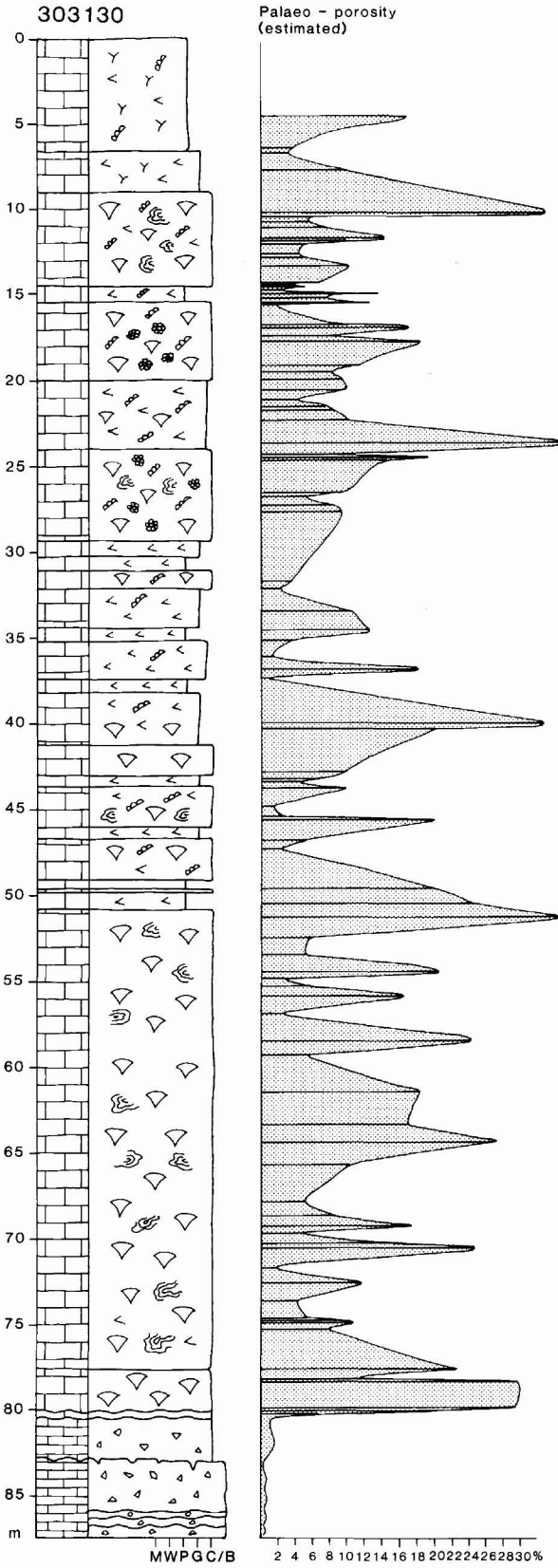
Fig. 8. Sedimentary log of core GGU 303130 with variations in estimated palaeo-porosity. Same symbols as Fig. 8.
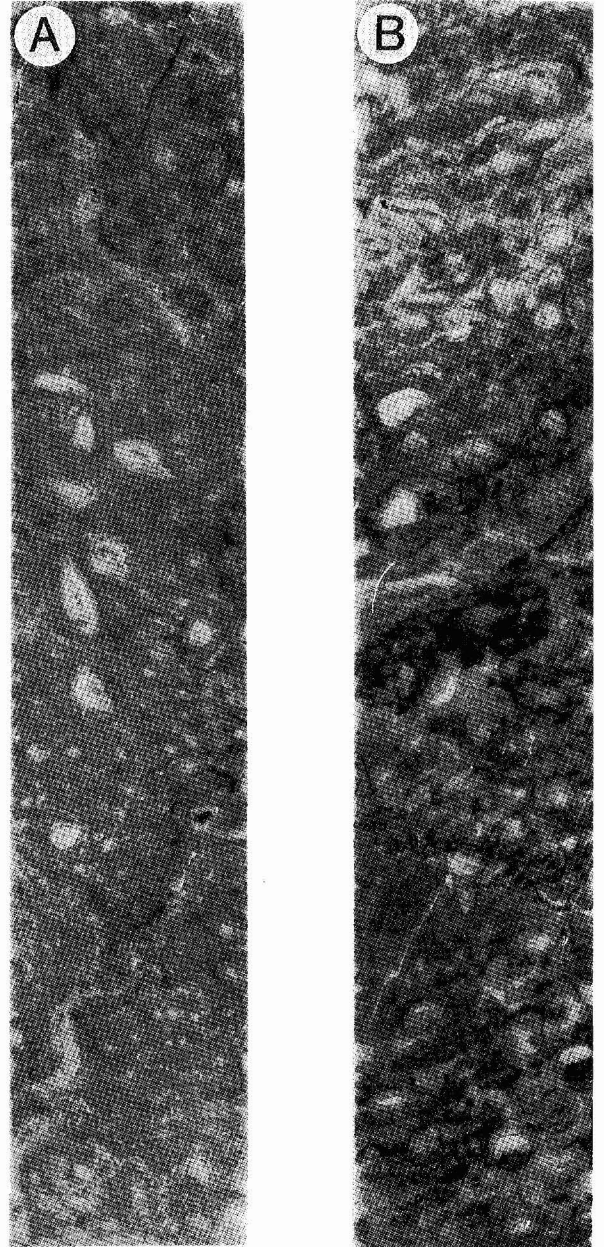

Fig. 9. Core pieces of bivalve-oncolite grainstone. (A) GGU 303129, 39.00–39.15 m. Note that large two shelled bivalves are filled with cement; (B) GGU 303129, 46.50–46,65 m. Note geopetal infill of some bivalves and abundant carbonate mud in the lower two-thirds of core.

9

Fig. 10. Thin-sections of bivalve-oncolite grainstone. (A) GGU 303129–51; facies dominated by thin-shelled bivalves. Note that the 'NW–SE' trending fracture is filled by two generations of cement. (B) GGU 303129–57; facies includes both thin-shelled bivalves and oncolites.
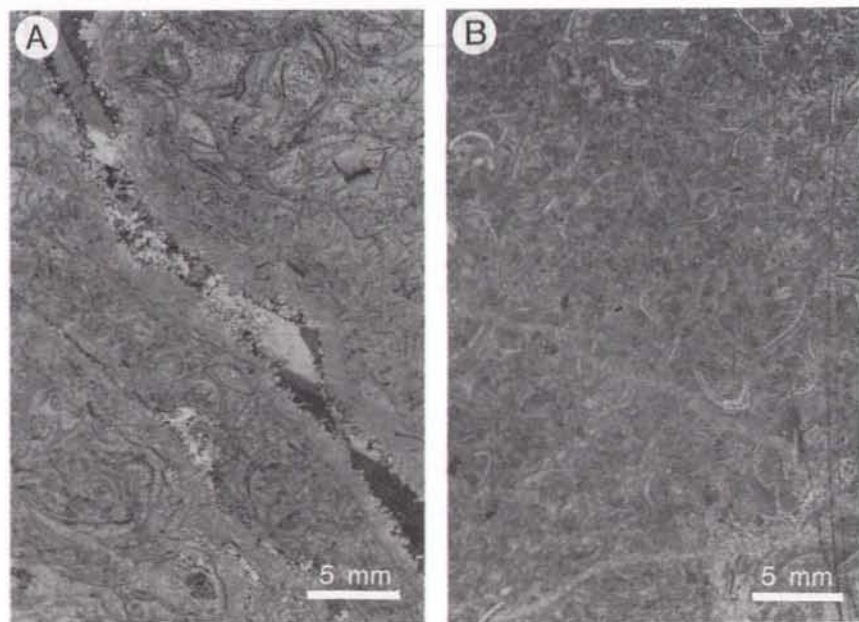
zones of square-tipped fibres, and as laminated or homogeneous layers of iron-poor calcite (Figs 13, 14; Plate 1, figs 1, 3; Plate 3, fig. 6). Early dissolution and fracturing is widespread and often fragments of cement-stone and cemented grainstone are incorporated in a later generation of marine cement (Fig. 13; Plate 1, figs 3, 4). This later marine cement is preserved as calcite with scalenohedral terminations (Plate 3, fig. 4). Also found in the brecciated parts of this facies is soil-like material implying that the brecciation and fracturing were related to subaerial exposure events and fresh-water flushing of the sediment. Late fractures, of which some are associated with the brecciation, are filled by marine cement (calcite with scalenohedral termina-tions) and/or equant calcite crystals.

This broadly defined facies represents deposition in a variety of shallow marine environments, all of which were characterised by conditions unsuitable to most marine life but extremely suitable for precipitation of aragonite.

Evidence of prolonged subaerial exposure is seen in the lower part of core GGU 303130 (50.8–80.6 m) both as a reddish iron-stained surface (80.2 m) (Fig. 12) and as extensive early fracturing and freshwater dissolution of aragonite cements followed by renewed marine ce-mentation (Figs 12, 13). In the upper part of core GGU 303130 (0–50.8 m) and in core GGU 303129 (34.0–53.0 m) fracturing is less pronounced, and freshwater flush-ing of this part of the mound is believed to be related primarily to later (?Permian or Permian–Triassic bound-ary) exposure of the entire mound.
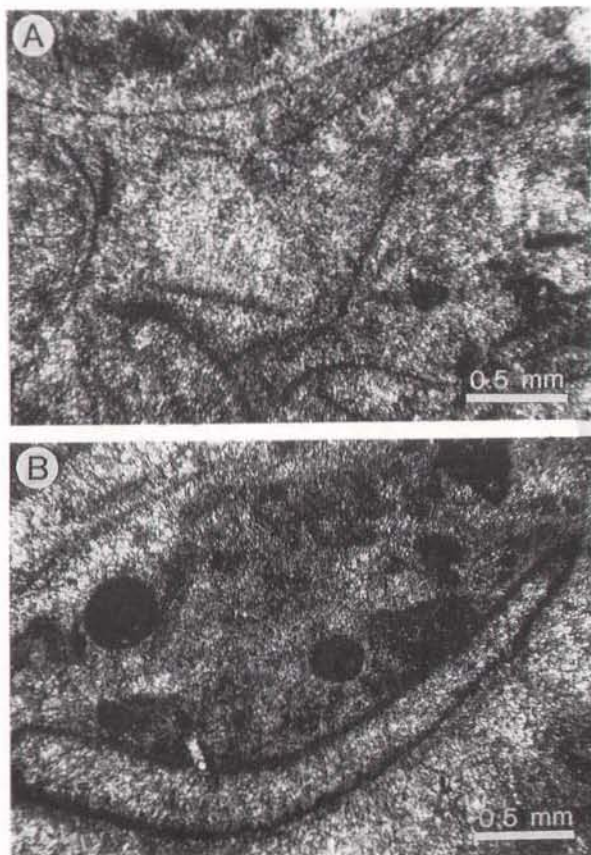

Fig. 11. Photomicrographs of bivalve-oncolite grainstone. (A) GGU 303129–48; thin-shelled bivalves overgrown by fibrous calcite cement. (B) GGU 303130–70 showing replacement of original shell by equant iron-poor calcite.
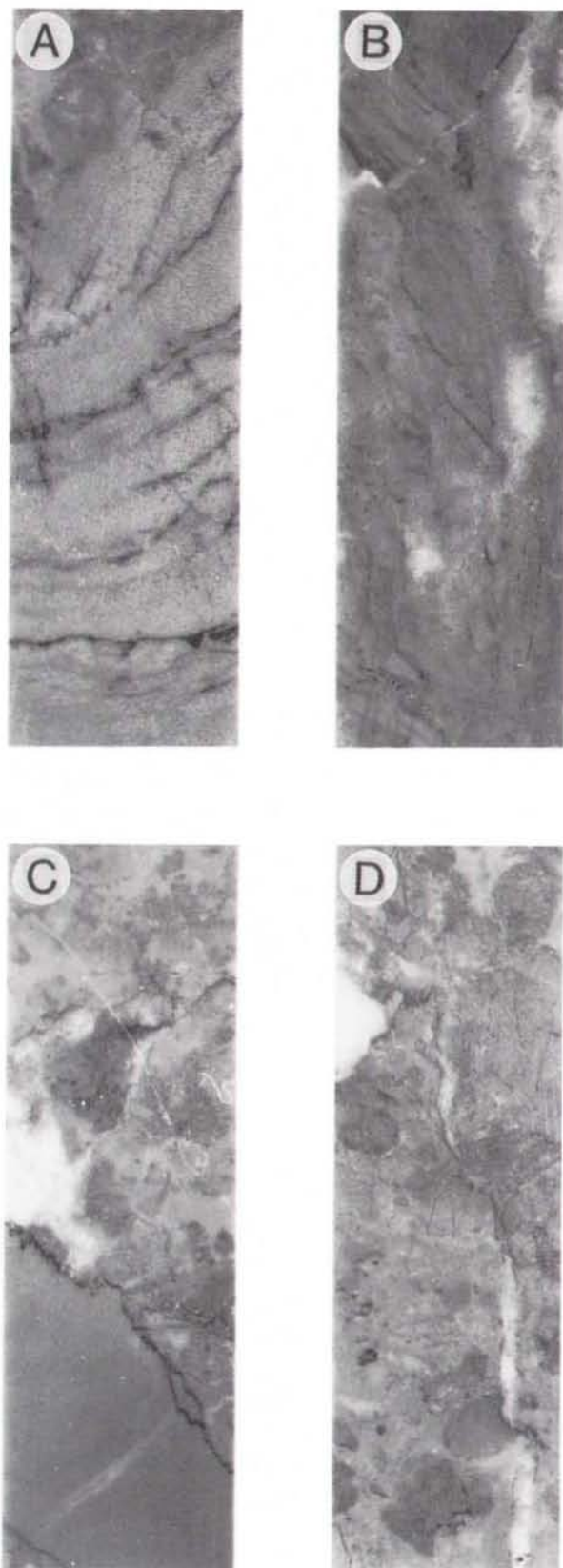
Fig. 12. Core pieces of marine cementstone. (A) GGU 303129, 38.10–38.20 m. Layers of laminated cement showing preferential dissolution of cement parallel to lamination (dark, oil-stained layers). (B) GGU 303130, 42.50–42.65 m. Laminated cement showing vertical growth of cement in (?) caves. (C) GGU 303130, 60.70–60.85 m. Laminated cement probably forming part of large botryoid overlain by cement-dominated bryozoan-foraminifer boundstone. (D) GGU 303130, 80.85–81.00 m. Fragments of marine cementstone cemented by 'later' marine cement.

Iron-rich, late calcite cements occur as fracture fill and as the latest diagenetic phase in solution-enlarged vugs (Fig. 13c; Plate 1, figs 1–4; Plate 2, figs 3, 4; Plate 3, figs 3–6).

Bryozoan-foraminifer boundstone. The dominant components in this facies are early marine cements, bryozoans and tubular foraminifers. Bryozoans and foraminifers together with encrusting algae appear to form the sedimentary frame within this facies (Figs 15, 16, 17). Locally bivalves form an important grain constituent in this facies but they are always encrusted by bryozoans and tubular foraminifers. Pervasive marine cementation stabilised the sediment, and this facies, together with the marine cementstones, formed the rigid core of the buildups.

Freshwater dissolution of aragonite cements and early fractures filled by iron-poor calcite are common features also in this facies (Fig. 16A). However, extensive brecciation and infill of soil-like material as seen in the marine cementstone, has not been recorded in this facies.

It is suggested that this facies was deposited in slightly deeper water conditions than the two previous facies, although still within shallow water. Marine conditions were mainly suitable for encrusting organisms, suggesting that the facies also represents deposition in a high energy environment. No evidence has been found indicating syndepositional subaerial exposure, and it is believed that this facies represents deeper marginal parts of the rigid buildups.

Iron-rich calcite cements occur mainly in fractures and solution-enlarged vugs (Fig. 16B).

Sedimentary evolution of the main buildups

The three facies previously described form the bulk of the buildup encountered in core GGU 303130 (Fig. 8). This 80 m thick buildup shows a distinctive vertical zonation of facies which was apparently controlled by water depths. The lower part is dominated by exten-
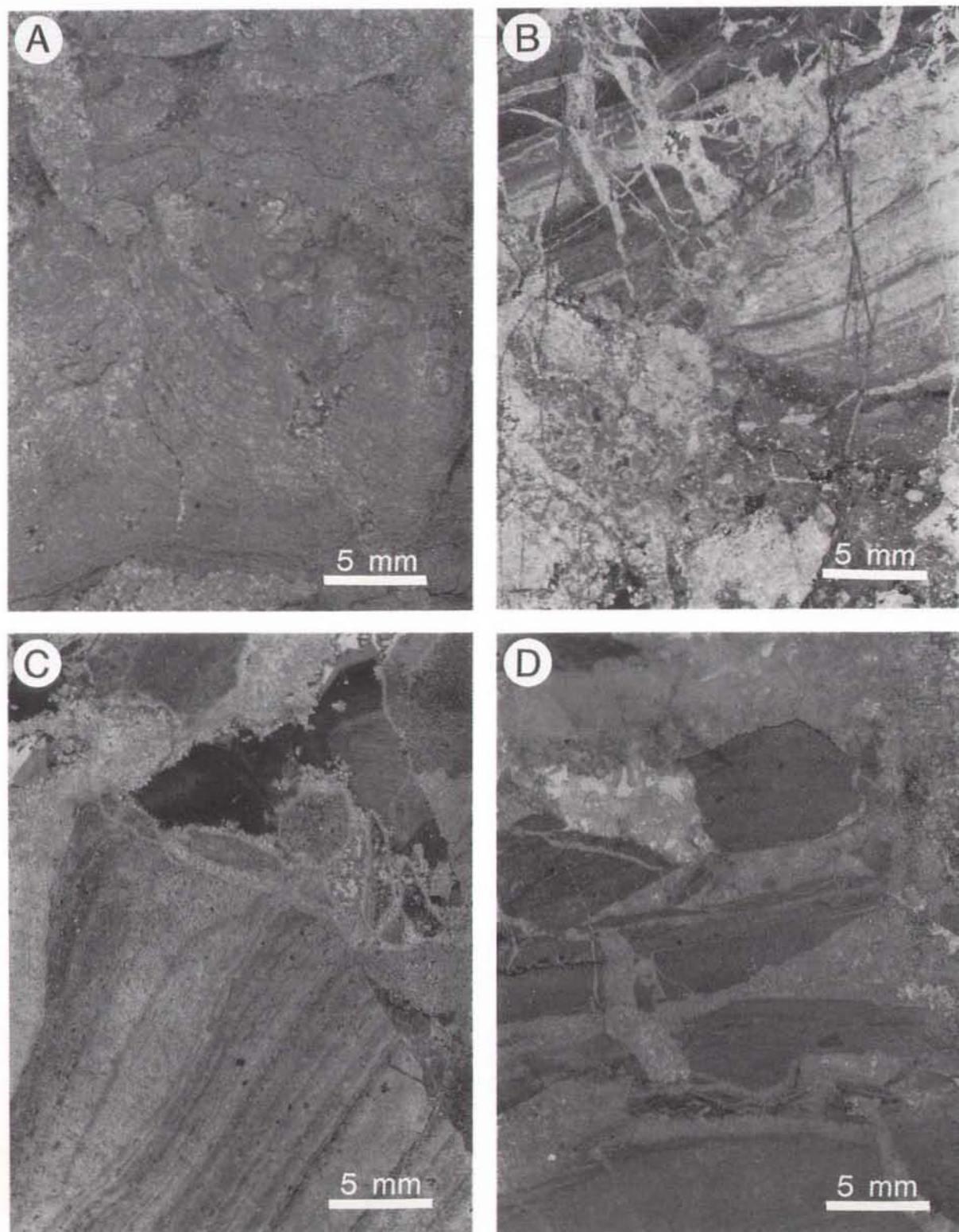
Fig. 13. Thin sections of marine cementstone. (A) GGU 303130–125; facies dominated by algae and encrusting organism of unknown affinity. (B) GGU 303130–111; intensely brecciated facies with laminated cement crusts cut by early fractures (light) and late fractures (dark). (C) GGU 303130–109; laminated cementstone fragments encrusted by marine calcite cement. Remaining pore space filled by coarsly crystalline (dark) calcite. (D) GGU 303130–91; fragments of marine cementstone encrusted by marine calcite cement. Note the pervasive early cementation post-dating first brecciation event.
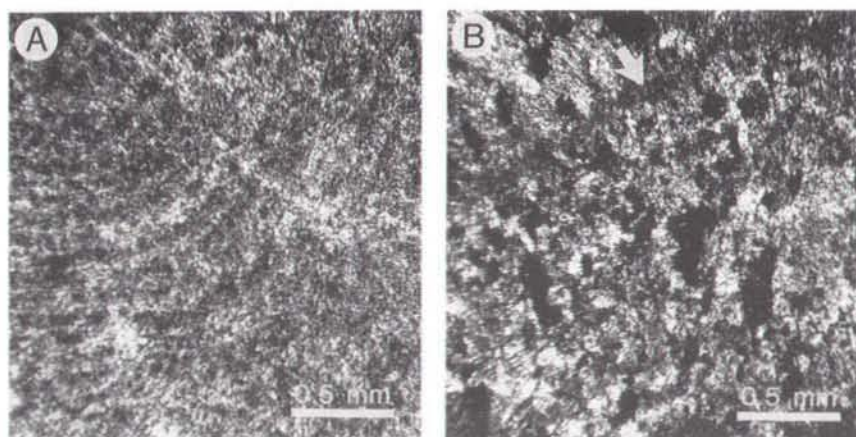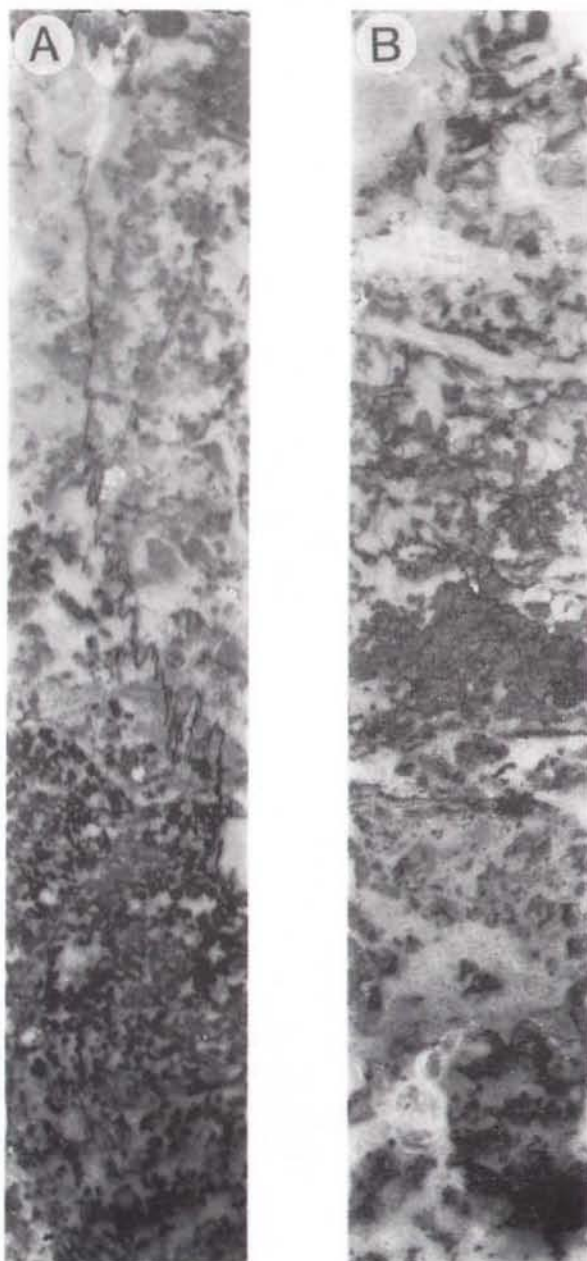
Fig. 14. Photomicrographs of marine cementstone. (A) Close up view of Fig. 13A showing algal lamination within the cement. Note cross-cutting early fracture. (B) GGU 303130–92 showing fan shaped crystals with uniform extension of calcite replacing aragonite botryoid. Note internal laminae of finely crystalline calcite within the botryoid (arrow).


sively brecciated marine cementstones with only minor bivalve grainstones. Deposition took place in a shallow marine, high energy environment, and several episodes of prolonged subaerial exposure of the mound crest took place during this early stage of development. The overlying part of the buildup is dominated by bryozoan-foraminifer boundstones with intervals of algae-dominated cementstone (Fig. 8). This zone probably represents slightly deeper water depositional conditions. The upper part of the core GGU 303130 is dominated by marine cementstones and bivalve-oncolite grainstones (Fig. 8) suggesting that a renewed shallowing took place.

The lower part of core GGU 303129 (34.0–53.0 m) is dominated by bivalve grainstones and marine cementstones with abundant algae. The core was drilled some distance away from the crest of the buildup, and the interval encountered most likely represents more marginal parts of the buildup than those seen in core GGU 303130.

The bryozoan cementstone facies suggested to form the main framework of the buildups (cf. Hurst *et al.*, 1989; Stemmerik *et al.*, 1989), has not been encountered in the two shallow cores. Most likely this facies formed in more protected parts of the buildup than those described above. The bryozoan cementstone facies is suggested to dominate the deeper, non-cored, parts of the investigated buildups and more deeply settled buildups as e.g. the Devondal buildup.

Fig. 15. Core pieces of bryozoan-foraminifer boundstone. (A) GGU 303130, 16.80–16.95 m. Lower half dominated by organic framework of bryozoans and tubular foraminifers (dark due to oil staining). Upper part with less dense organic frame but abundant marine cement. (B) GGU 303130, 18.50–18.65 m. Note rapid changes in relative contribution of marine cement and organic components.

Fig. 16. Thin sections of bryozoan-foraminifer boundstone. (A) GGU 303130–32; facies dominated of encrusting bryozoans and tubular foraminifers. Note intensive fracturing entirely cemented by early diagenetic calcite (arrows) and widespread hydrocarbon preservation in moulds after tubular foraminifers. (B) Facies dominated by bryozoans, tubular foraminifers and algae (seen as vauge often vertical lamination (arrows). Note that most fractures are filled mainly by late diagenetic coarsely crystalline calcite (dark).
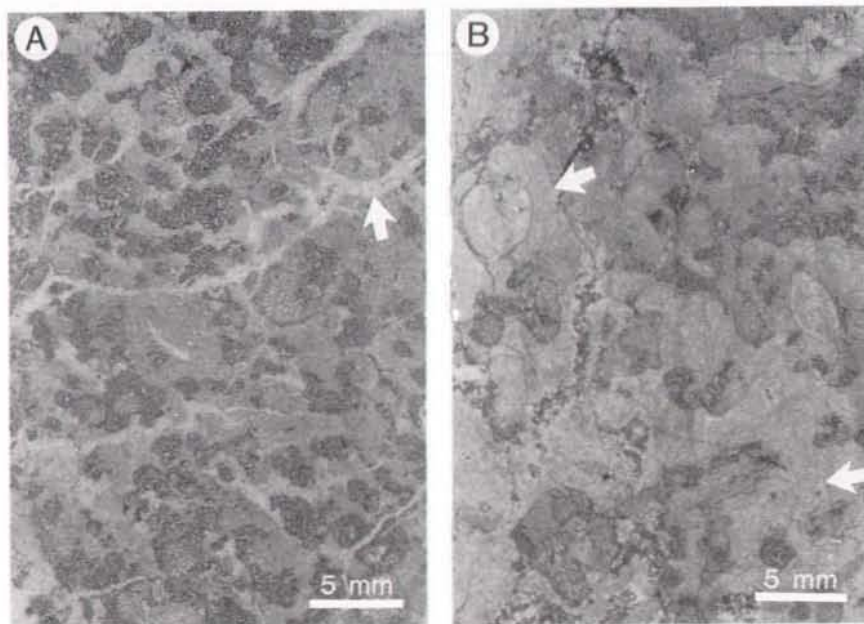
Flank deposits

The flank deposits surrounding the rigid frame of the buildups are mainly composed of resedimented shell debris, and include bryozoan, brachipod and crinoid-dominated grainstones, packstones and wackestones (Surlyk et al., 1986; Hurst et al., 1989; Stemmerik & Hurst, unpublished manuscript). Small bryozoan mounds also occur in this setting as downward prograding units encased in debris deposits (Fig. 6) (Hurst et al., 1989). The following facies descriptions are based entirely on material from core GGU 303129; sediments in core GGU 303117 are dominantly packstones with few intervals of bryozoan cementstones.

Bivalve-bryozoan packstone. This facies is dominated by bivalves and bryozoans (Figs 18, 19, 20). Carbonate mud occurs in various amounts and usually the sediment can be characterized as a packstone (cf. Dunham, 1962). However, at certain intervals early marine cement is an important rock-forming constituent, and in some intervals vadose, equant calcite cements dominate (Fig. 19A). This facies differs from the bivalve-dom-
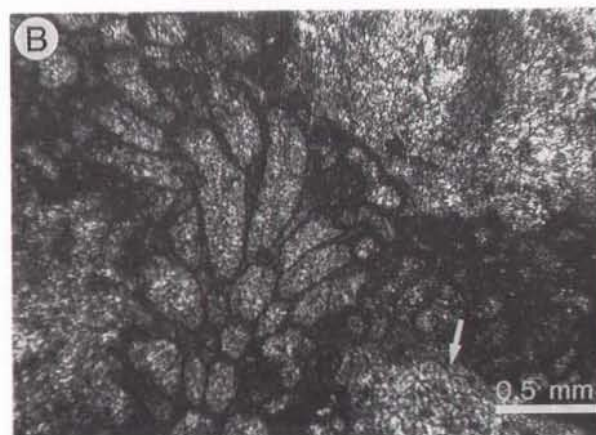
Fig. 17. Photomicrographs of bryozoan-foraminifer boundstone. (A) GGU 303130–29; tubular foraminifer encrusted by vaguely laminated marine cement. Note that most primary shell material is leached and that the mould is now filled by hydrocarbons. (B) GGU 303130–33; bryozoan encrusted by tubular foraminifers. Note growth of foraminifers on grain of unknown affinity (arrow) which was leached and cemented by early diagenetic calcite prior to leaching of the foraminifers.

Fig. 18. Core pieces of bivalve-bryozoan packstone with dominance of bryozoans and small bivalves. Note uneven distribution of marine cement (light) and carbonate mud (dark). GGU 303129, 16.20–16.35 m.

inated facies in the frame of the buildup in having a significantly higher content of bryozoans.

The facies represents the proximal parts of the flank deposited during stages when the buildup was dominated by faunas of bivalves and bryozoans. The intervals richer in cement may represent small prograding mounds formed along the margins of the main buildup.

Replacement of the aragonitic bivalves by equant

calcite cement, partial dissolution of marine aragonite cements, and rare early fractures all indicate that this facies also was diagenetically modified in a freshwater regime.

Bryozoan-foraminifer packstone. The dominant constituents in this facies are *Acanthocladia*-like bryozoans, small foraminifers (*Nodusaria* and *Agathammina*) and brachiopods. Carbonate mud occurs in variable amounts as also does marine cement (Figs 21, 22, 23).

This facies is suggested to represent proximal flank deposits formed during a stage of buildup growth when bryozoans dominated the buildup frame, and thus deeper water conditions than the previous facies. Also, this facies shows diagenetic modifications indicative of freshwater diagenesis.

Sedimentary evolution of the flank deposits

The flank deposits in core GGU 303129 (0–34.0 m) show an upward deepening trend; the lower half of this interval is dominated by bivalve-bryozoan packstones and grainstones while the upper part is composed of bryozoan-foraminifer packstones (Fig. 7). This evolution is comparable to that seen in core GGU 303130 with the exception of a final upward shallowing stage. However, a final shallowing event has also been described from the flank deposits surrounding the Devondal buildup (Hurst *et al.*, 1989).

Diagenesis

Based on petrography and isotope geochemical evidence from cores GGU 303129 and GGU 303130 several diagenetic phases (seen as dissolution events and different generations of calcite cements) can be distinguished. Similar diagenetic modifications have been recognized elsewhere in the area (Scholle *et al.*, in press), and it is therefore suggested that the main diagenetic phases are of regional significance.

The diagenetic modifications can be related to two distinctive events, the first syn-depositional to early post-depositional, the second late burial, post-hydrocarbon migration and most likely of Tertiary age (cf. Christiansen *et al.*, 1990).

Early diagenesis

Early diagenesis includes precipitation of various iron-poor calcite cements, partial dissolution of aragonite, fracturing and brecciation of the sediment, and possibly also calcite replacement of undissolved arago-

Fig. 19. Thin sections of bivalve-bryozoan packstone. (A) GGU 303129–31; lower part packstone with bryozoans, bivalves and carbonate mud (dark), upper part with less mud and extensive marine cement on bivalves. (B) GGU 303129–32; facies dominated by large bivalves and fragments of *Acanthocladia*-type bryozoans.
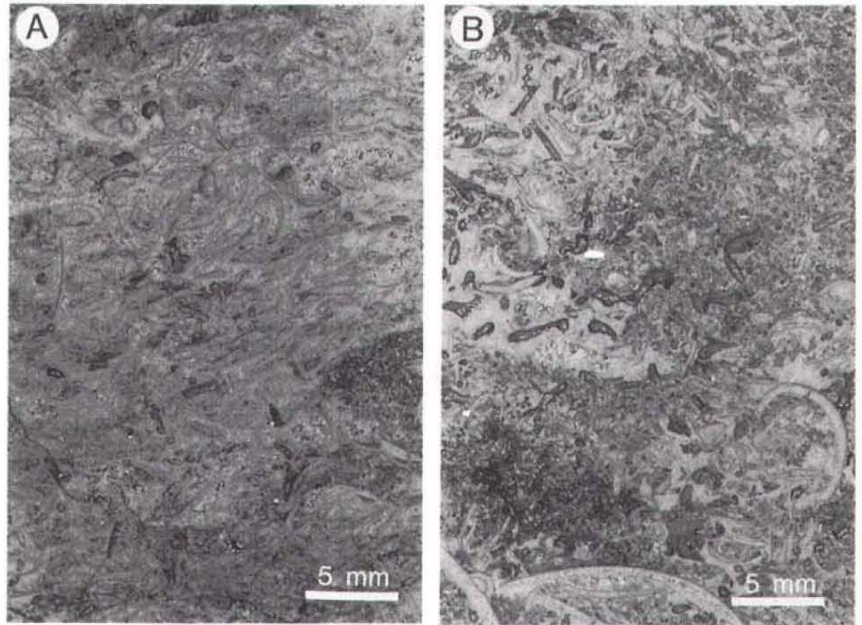
Fig. 20. Photomicrograph of bivalve-bryozoan packstone showing replacement of primary bivalve shells by equant iron-poor calcite. Dark material on bivalve shells consists of encrusting foraminifers. GGU 303129–32.

Fig. 21. Core pieces of bryozoan-foraminifer packstone. (A) GGU 303129, 6.80–6.95 m. Facies dominated of bryozoans with scattered foraminifers (arrows) and brachiopods. Note geopetal infill in brachiopod. (B) GGU 303129, 9.80–9.95 m. Note abundant oil-stained stylolites. Facies dominated by bryozoans.

Fig. 22. Thin sections of bryo-zoan-foraminifer packstone. (A) GGU 303129–12; facies dominated of bryozoans, brachiopods and small foraminifers. Note geo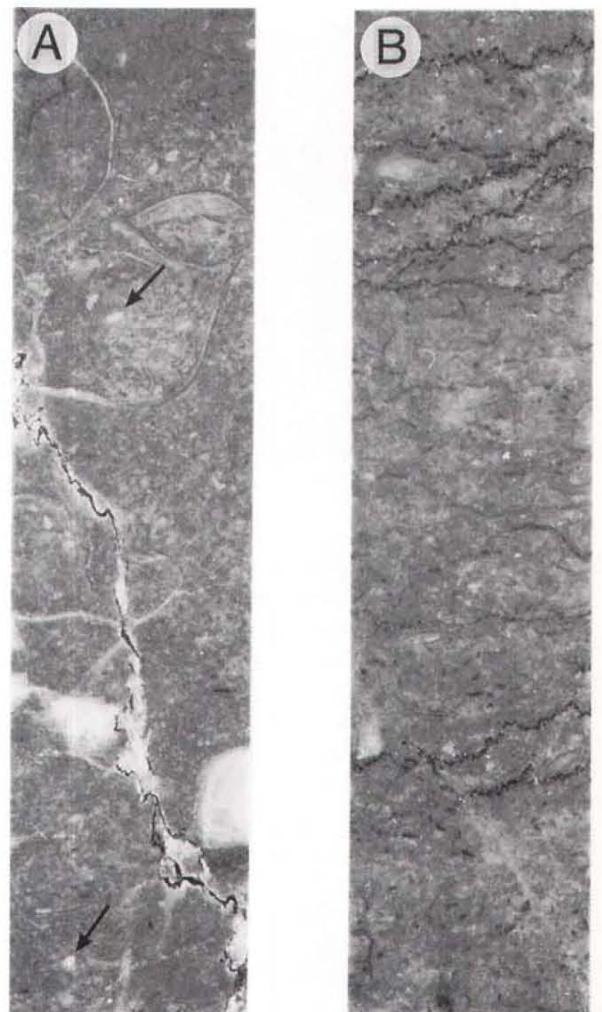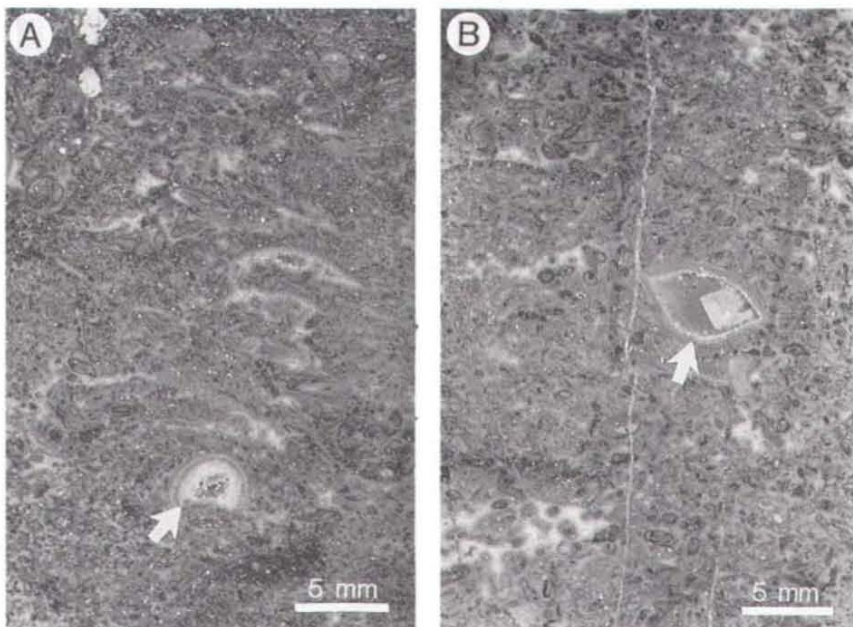petal infill in brachiopods (arrow) followed by a generation of early iron-poor calcite (light) and late iron-rich calcite (dark). (B) GGU 303129–13; facies dominated by bryozoans and foraminifers. Note cross-cutting fractures filled with early cement and brachiopod filled with two generations of cement (arrow).
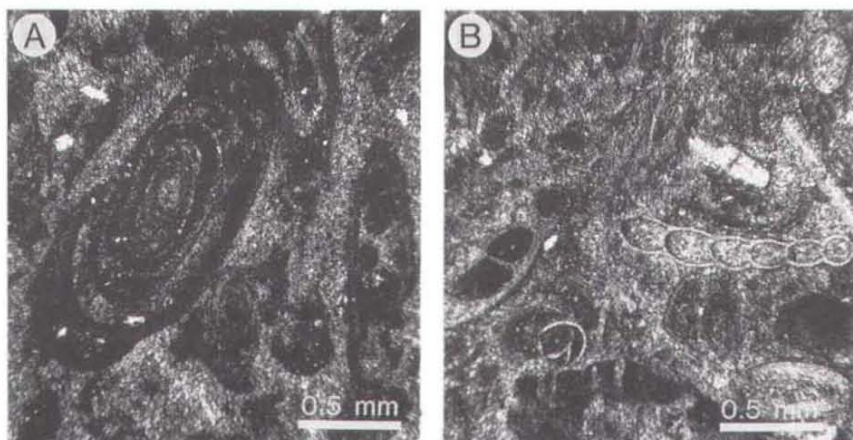

Fig. 23. Photomicrographs of bryozoan-foraminifer packstone. (A) *Nodusaria*-like foraminifer and *Acantocladia*-like bryozoans, GGU 303129–14. (B) *Agathammina*-like foraminifer, GGU 303129–12.

nite. The following diagenetic stages have been recognized in the buildups south of Paradigmabjerg:

(1) Marine precipitation of aragonite to form laminated and homogeneous cement crusts and botryoids (Plate 1, figs 1, 3; Plate 3, fig. 6).

(2) Early freshwater dissolution of parts of the aragonite cement and all aragonitic shell material (Plate 1, figs 1–4; Plate 3, fig. 6). This dissolution event is recognized also by deposition of soil-like material in fractures (Fig. 24). This event is restricted to the buildup crest facies during early stages of growth.

(3) Post-dissolution marine cementation in fractures and solution enlarged pores (Plate 1, figs 3, 4; Plate 3, fig. 4), and aragonite cementation as botryoids and crusts in the growing buildups.

(4) Renewed freshwater dissolution of aragonite and creation of a new generation of fractures. This event possibly post-dates buildup growth and also involved precipitation of equant calcite cements and calcite replacement of aragonite, all believed to have occurred in a freshwater phreatic diagenetic environment. This latter proposition is based on carbon and oxygen isotope studies of the various types of cement. Iron-poor calcite cements generally have $\delta\ ^{13}C$ values in the range 4–6‰ PDB, and $\delta\ ^{18}O$ values ranging from -9 to -11‰ PDB (Fig. 25). The relatively heavy $\delta\ ^{13}C$ values are typical for marine, Upper Permian components; the $\delta\ ^{18}O$ data show an isotopic shift towards lighter oxygen values, indicating stabilization in meteoric waters (e.g. Scholle *et al.*, in press).
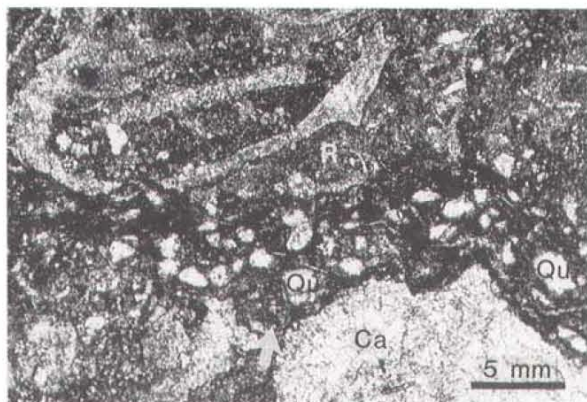
Fig. 24. Soil-like material filling part of early fracture. Ca is calcite cement, Qu quartz grains in micritic material, and R original sediment. Arrow points towards lower margin of fracture.

Fig. 25. Cross-plot of carbon and oxygen isotopic values of cements from cores GGU 303129 and GGU 393130.

Late diagenesis

The late diagenetic calcite is typically coarsely crystalline, iron-rich and displays highly negative $\delta^{18}O$ values in the range -11 to $-20‰$ relative to PDB; $\delta^{13}C$ values are from 0 to 4‰ relative to PDB (Fig. 25). Associated with these cements are commonly fluorite, baryte, galena and quartz (Plate 2, figs 3, 4; Plate 3, fig. 2). The calcite ranges from being moderately iron-rich (violet in thin-sections stained with alizarin-red and ferrocyanid using stage I and II in the method described by Dickson (1965) – see Plates 1–3) to extremely iron and manganese-rich (blue in stained thin-sections – see Plates 1–3). Blue stained cements from the Devondal buildup were reported to have an average of more than 1.5% Fe and 1.1% Mn (Surlyk et al., 1986; Scholle et al., in press).

The highly negative $\delta^{18}O$ values of these late cements together with fluid inclusion data from associated fluorite and quartz indicate formation temperatures of 115–150°C (cf. Harpøth et al., 1986; Surlyk et al., 1986). The few available fission-track data from the area indicate that immediately after heating there was a rather rapid uplift through the 100°C isotherm approximately 20 Ma ago (cf. Fig. 26) (Hansen, 1988). This implies a Tertiary age for the late diagenetic, iron-rich cements and associated minerals.

Porosity evolution

Petrographic examination of the relationships between hydrocarbons which migrated into the buildups and the different generations of cement shows that the precipitation of most of the late diagenetic, iron-rich cements and associated minerals post-dates migration of hydrocarbons (Plate 2, fig. 3; Plate 3, figs 1, 3, 5) (Hurst
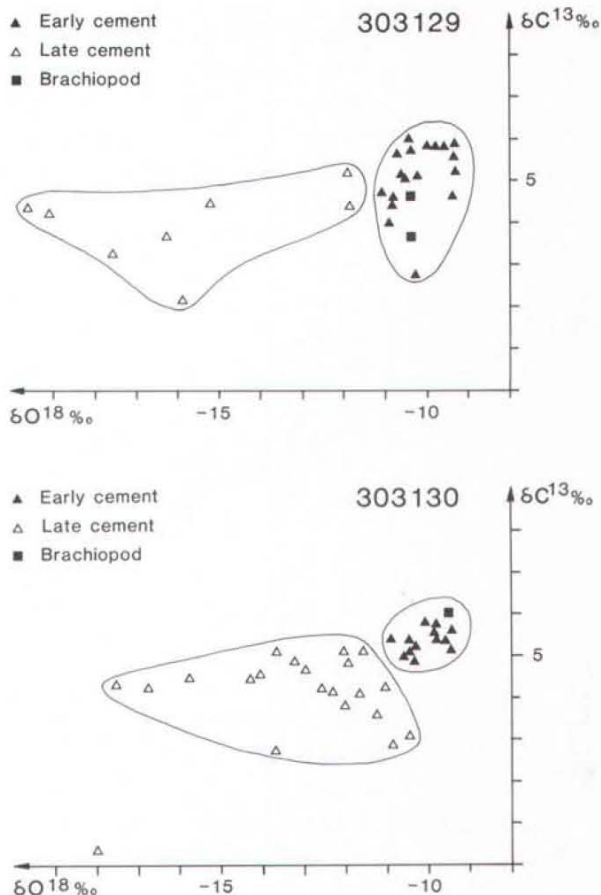
et al., 1989; Scholle et al., in press). In the early cemented parts of the buildups, i.e. the main frame and the proximal flank deposits, pore space available for migrating hydrocarbons was thus controlled mainly by early diagenetic processes, as compaction during burial was negligible. In contrast, the more distally deposited, mud-dominated flank deposits were compacted during burial, and the primary, depositional porosity was gradually reduced to eventually become almost zero. The reservoir potential of the distal flank deposits is therefore dependent on the timing of hydrocarbon migration in relation to burial, and it is likely to be poor if hydrocarbons have to be sourced by the Upper Permian Ravnefjeld Formation shales (cf. Fig. 26). However, if stratigraphically deeper, earlier-matured source-rocks occur in the basin, the flank deposits may have a fair reservoir potential.

The evolution of porosity in the early cemented parts of the buildups is controlled by two opposing processes: early marine and freshwater cementation occluding po-
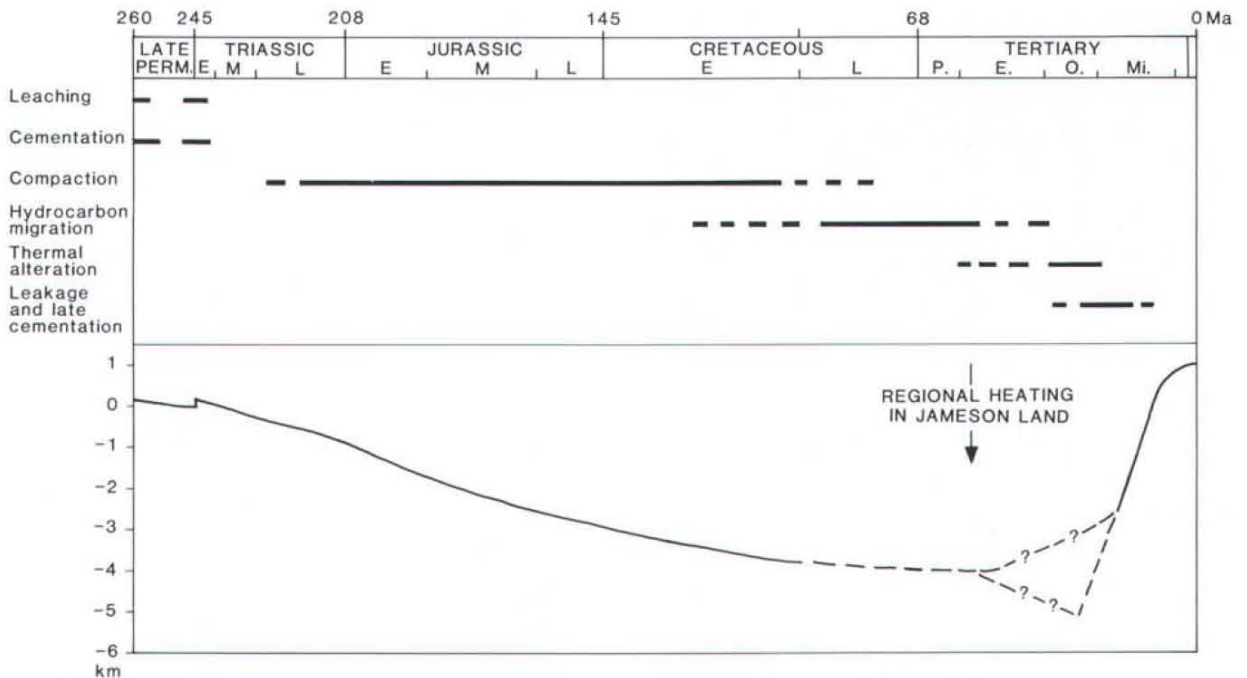
Fig. 26. Burial history of the Upper Permian sediments in Wegener Halvø showing proposed timing of different diagenetic events. Burial history based on the cummulative thickness of younger units as recorded by Surlyk *et al.* (1973), Clemmensen (1980) and Marcussen *et al.* (1987).

rosity, and early freshwater leaching creating new porosity. The pervasive marine cementation of the buildup frame means that initial (essentially syn-depositional) porosity was close to zero. Creation of new pore space and improvement of the reservoir capacity is therefore entirely dependent on early, freshwater leaching of aragonite, and therefore the best reservoirs are expected to be found on structural highs where the buildups more often became subjected to exposure.

According to the porosity evolution outlined all pores available during hydrocarbon migration are of secondary origin. Most pores are non-fabric selective fracture and vug type pores, using the classification of Choquette & Pray (1970). However, in the bryozoan-foraminifer boundstone facies fabric selective moldic pores dominate (Plate 2, fig. 1).

Reservoir evaluation

Evaluation of the reservoir potential of the Upper Permian buildups in the Jameson Land basin is based on the assumptions that (1) the early diagenetic history of the buildup in Wegener Halvø is representative for buildups in more basinal settings; (2) late diagenetic cementation and expulsion of hydrocarbons from the buildups did not occur in the basin, but is restricted to Wegener Halvø and other severely uplifted areas (cf.

Fig. 26), and (3) the relative proportions of the different facies seen in Wegener Halvø are representative for the basin.

Palaeo-porosity estimates

Estimates of the palaeo-porosity (defined as porosity prior to hydrocarbon migration) of the buildups in Wegener Halvø are based on the assumption that the effective porosity at the time of hydrocarbon migration can be estimated by adding the volumes of late diagenetic cement, associated late minerals and dead hydrocarbons to the present day porosity. This implies that all late cement was infill in pre-existing pores. This is however somewhat questionable as part of the cement fills fractures, and may rather represent 'pore space' created during the expulsion of the hydrocarbons.

Methods. The palaeo-porosity is estimated on the basis of thin-section analysis as the composite area of present day porosity, late diagenetic minerals and dead hydrocarbons as percentage of the total area of the section.

More than 200 thin-sections were analysed by using the image analysis system at the Geological Survey of Denmark (DGU) to discriminate the late diagenetic minerals and the dead hydrocarbons from the rock-forming iron-poor calcite. The thin-sections were
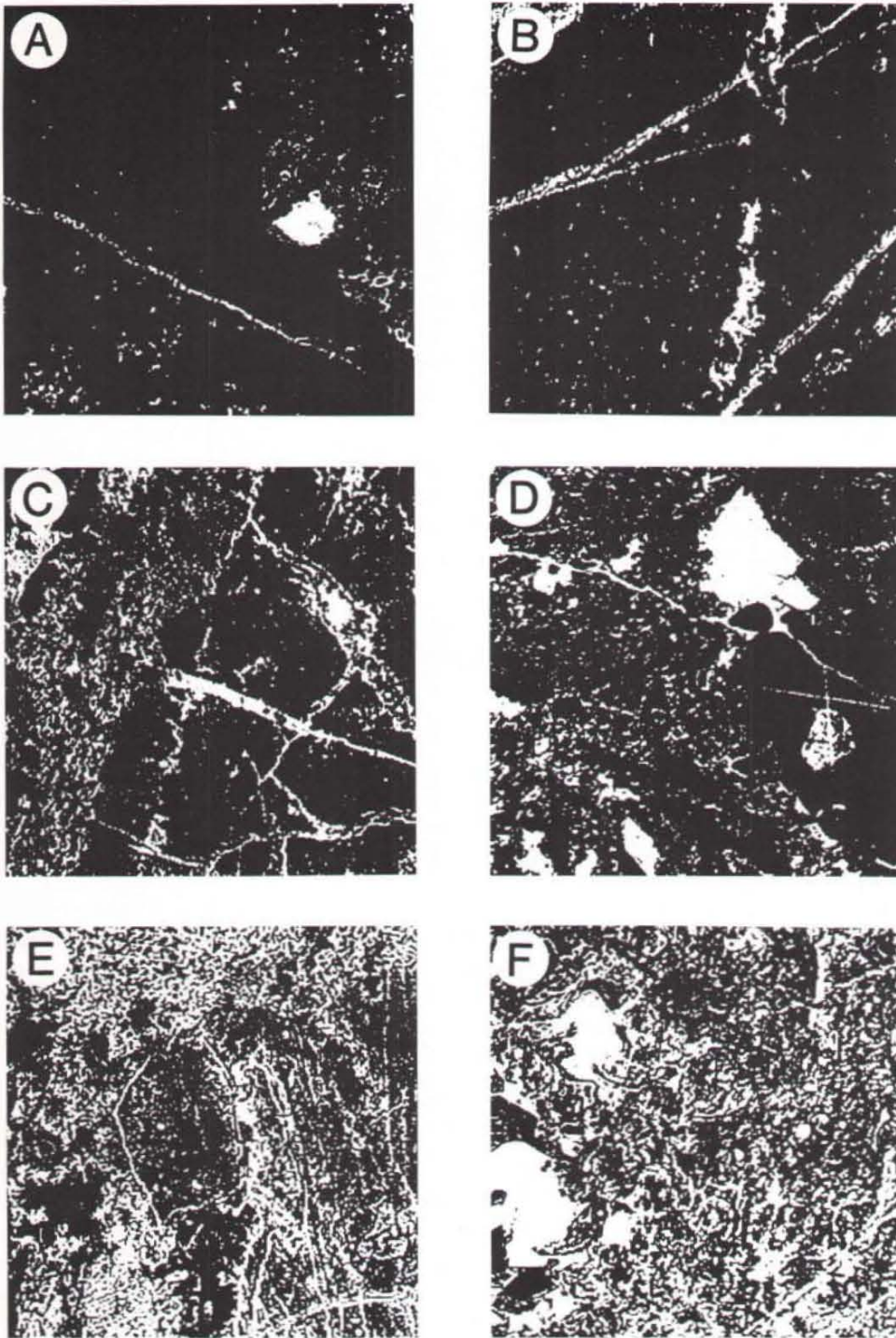
Fig. 27. Examples of palaeo-porosity distribution using image analysis and the methods described in the text; (A) GGU 303130–129 4% estimated porosity; (B) GGU 303130–21 7% estimated porosity; c) GGU 303130–102 17% estimated porosity; (D) GGU 303130–74 18% estimated porosity; (E) GGU 303130–91 36% estimated porosity; (F) GGU 303130–41 38% estimated porosity.

stained by alizarin-red and ferricyanide, to differentiate between iron-poor calcite (red-stained) and iron-rich calcite (bluish-stained) (see Plates 1, 2, 3). Thin-sections were photographed at a 1:1 scale, and the colour prints were used for image analysis.

The DGU image analysis configuration has the analogous signal generated in a TV-scanner mounted on a microscope. The signal is digitized in a analog/digital converter and stored in a 2 Mb image memory with a spatial resolution of 512–512 pixels and a grey value resolution of 8 bits (256 grey values). The image manipulation is carried out by microprogram orders, the programming is menu oriented and is controlled via the keyboard and/or the digitizer Tablet. The image analyser was programmed to select the grey values of blue stained cement and dead hydrocarbons. Before measuring, the automatically selected areas were displayed on a monitor (Fig. 27) and were visually controlled. This method is time saving but has some minor disadvantages, particularly when analysing mud-rich sediments as the carbonate mud displays almost the same grey values as dead hydracarbons. To avoid this problem, the programme allows, in addition to the automatic selection of grey values, manual selection of grey values to ensure the best possible fit.

Results. The estimated palaeo-porosity values and their variation within the investigated shallow cores are given in figures 7 and 8. The average palaeo-porosity is 5.0% in core GGU 303117, 5.4% in GGU 303129 and 11.9% in GGU 303130.

The highest estimated palaeo-porosity was found in the marine cementstones in the lower part of core GGU 303130. The interval from 51.8–80.5 m has an average palaeo-porosity of 14.2% compared to 9.8% for the marine cementstones and bryozoan-foraminifer boundstones higher up in the core. The bivalve-oncolite grainstones have an estimated average palaeo-porosity of 8.0%.

The estimated palaeo-porosity values for core GGU 303130 are significantly higher than those in core GGU 303129 (Table 1), even when compared facies by facies. The main difference between the two cores is the intense fracturing seen in GGU 303130. Dating of these fractures in relation to hydrocarbon migration has not been unequivocally established but most likely some fractures post-date hydrocarbon migration. However, many fractures have a more complex cementation history that clearly shows that they started as early, syndepositional fractures. These fractures did most likely represent pores during times of hydrocarbon migration.

Core GGU 303117 displays highly variable palaeo-porosity values ranging from almost no porosity in the

Table 1. *Estimated and measured palaeo-porosity values in the Wegener Halvø Formation buildups*

	Main buildup	Proximal flank
303129 (average)	5.4%	5.4%
303130 (average)	11.9%	-
303117 (average)	-	~ 5.0%
Brecciated marine cementstone	14.2%	-
Bryozoan-foraminifer boundstone	9.8%	-
Bivalve-oncolite grainstone	8.0%	-
Estimated average	10%	5-6%
Measured	7.1%	5.4%

mud-dominated facies to average values of 5–6% in the early cemented, more proximal facies.

In general, the results indicate that the porosity distribution within the buildups and associated sediments at the time of hydrocarbon migration was highly heterogeneous. The distal, mud-rich flank deposits apparently had been compacted to have no porosity left. More proximal flank deposits are suggested to have had a palaeo-porosity between 5 and 6%, while the brecciated marine cementstones in the central buildups appear to have had a somewhat better palaeo-porosity, possibly more than 10% (Table 1). This palaeo-porosity distribution is confirmed by analyses of carbonate rocks saturated with dead hydrocarbons (Springer, 1989). The measured palaeo-porosities of cleaned samples of proximal flank deposits and marine cementstones average 5.4% and 7.1% respectively. The value for the cementstones, however, may be higher than measured as most porosity occurs as vugs (Springer, 1989).

Reservoir capacity

Reservoir facies within the Wegener Halvø Formation buildups on Wegener Halvø are restricted to the main buildup and the proximal parts of the flank deposits.

The palaeo-reservoir volumes of the three investigated buildups were estimated using a palaeo-porosity of 10% for the buildup facies and 5% for the proximal flank deposits. Thickness and area of the different facies are based on field observation; it is assumed that only flank deposits within a distance of 100 m from the main buildup have reservoir potential. The estimated volume, expressed as all available palaeo-pore space within the buildups, ranges from approximately 100 000 m^3 in the southern Paradigmabjerg buildup to 1 400 000 m^3 in

Table 2. Estimated reservoir volume of the Wegener Halvø Formation buildups in Wegener Halvø

	Main buildup m³	Proximal flank m³	Total m³
Devondal	1 250 000	150 000	1 400 000
Paradigmabj N	71 500	110 000	181 500
Paradigmabj S	44 000	55 000	99 000
Wegener Halvø trend	-	-	13 500 000

the Devondal buildup (Table 2). The Wegener Halvø trend, including all buildups in the area (Fig. 2), has an estimated palaeo-reservoir capacity of approximately 13 500 000 m³ (85 × 10⁶ Bbl) over an area of 60 km².

Implications for the Jameson Land basin. At present the minimum field size considered economic in the basin is close to 160 × 10⁶ m³ (1 × 10⁹ Bbl) recoverable oil. This figure is 40 to 50 times larger than that estimated for the entire Wegener Halvø trend, and obviously this type of carbonate platform development with scattered buildups is not a potential reservoir target within the basin.

Two major differences affecting the reservoir potential of the Wegener Halvø buildups may be expected in the basin: increased buildup thickness and increased buildup density. Within the Wegener Halvø area there is a trend towards thicker and more densely spaced buildups towards the south (Fig. 2). (Stemmerik *et al.*, in press). This trend is expected to continue towards the basin so that thicker carbonate platforms with more closely spaced buildups or probably even barrier reef-type developments may occur in the basin. Proof of the existence of such platforms and comparison of their diagenetic history to that outlined for the basin margin buildups must, however, await drilling in the basin.

Discussion

Most Upper Palaeozoic bryozoan-dominated buildups are associated with extensive precipitation of early marine cement (e.g. Tucker & Hollingworth, 1986; Beauchamp, 1989; Davies *et al.*, 1989; Stemmerik, 1989) which ultimately occludes most primary porosity. The reservoir potential of this type of buildup is therefore dependent on later diagenetic modifications.

The creation of reservoir properties in the Wegener Halvø Formation buildups in the Wegener Halvø area appears to be related to early (intra-Upper Permian

and/or Permian–Triassic boundary) leaching of aragonite due to freshwater flushing during subaerial exposure; no evidence of early dolomitization of the buildups, such as recorded in the Zechstein basin of North-West Europe (Füchtbauer, 1980; Smith, 1981; Hollingworth & Tucker, 1986), has been seen. While the diagenetic history of the exposed buildups along the basin margin is fairly well documented, problems may occur when extrapolating these processes to subsurface buildups. However, carbonate platforms and buildups tend to build to sea-level, and it is therefore expected that also carbonates nearer the centre of the basin will become subaerially exposed during lowering of sea-level.

Summary and conclusions

The occurrence of bryozoan-submarine cement buildups in the Wegener Halvø area is controlled by the morphology of the karst surface of the Karstryggen Formation.

The main buildups are composed of bivalve-oncolite grainstone, marine cementstone and bryozoan-foraminifer boundstone. The main rock forming agents were marine cement, algae, bryozoans and tubular foraminifers.

The flank deposits surrounding the buildups are composed of various types of grainstones, packstones and wackestones. The fauna includes bryozoans, brachiopods, crinoids and foraminifers.

Early diagenetic processes include precipitation of iron-poor calcite cements, partial dissolution of aragonite, fracturing and brecciation, and possibly replacement of aragonite by calcite.

Late diagenetic processes include precipitation of iron-rich, coarsely crystalline calcite, fluorite, baryte, galena and quartz. Formation temperatures were in the range of 115–150°C. In non-cemented flank deposits late diagenesis also includes compaction and pressure solution.

The late diagenetic cement post-dates hydrocarbon migration and is most likely of Tertiary age. Thus palaeo-porosity, defined as porosity at time of hydrocarbon migration, can be estimated by adding volume of late diagenetic minerals to present-day porosity.

Palaeo-porosity is estimated by image analysis to be c. 10% in the main buildups and 5–6% in the proximal flank deposits. These values may be overestimated as many fractures filled by late diagenetic minerals have not been properly dated with respect to hydrocarbon migration.

The reservoir capacity of the exposed buildups in the Wegner Halvø area is estimated to be in the range 0.1 ×

10^6 m^3 to 1.4×10^6 m^3 with a cummulative capacity of 13.5×10^6 m^3 for the entire buildup trend covering approximately 60 km^2.

The estimated reservoir capacity of the buildup trend is 40–50 times smaller than the economically defined minimum field size in the area, and therefore this type of carbonate platform with scattered buildups appears to be non-prospective in this region.

Buildups towards the centre of the basin are, however, expected to be thicker and more continuous than those seen along the basin margin, and they may form bodies sufficiently large to provide the necessary reservoir volume.

The potential of basinal buildups as reservoirs is dependent on diagenetic modifications similar to those recorded in the basin margin buildups, as no evidence of early dolomitization of any part of the Wegener Halvø Formation has so far been documented.

References

Beauchamp, B. 1989: Lower Permian (Sakmarian) *Tubiphytes*-bryozoan build-ups, southwestern Ellesmere Island, Canadian Arctic Archipelago. *In* Geldsetzer, H. H. J., James, N. P. & Tebbutt, G. E. (ed.), Reefs – Canada and adjacent areas. *Mem. Can. Soc. Petrol. Geol.* **13**, 585–589.

Choquette, P. W. & Pray, L. C. 1970: Geological nomenclature and classification of porosity in sedimentary carbonates. *Bull. Amer. Assoc. Petrol. Geol.* **54**, 207–250.

Christiansen, F. G. & Stemmerik, L. 1989: Shallow core drilling of Upper Permian and Upper Triassic – Lower Jurassic potential reservoir rocks in central East Greenland. *Rapp. Grønlands geol. Unders.* **145**, 79–84.

Christiansen, F. G., Piasecki, S. & Stemmerik, L. 1990: Thermal maturity history of the Upper Permian succession in the Wegener Halvø area, East Greenland. *Rapp. Grønlands geol. Unders.* **148**, 109–114.

Clemmensen, L. B. 1980: Triassic lithostratigraphy of East Greenland between Scoresby Sund and Kejser Franz Josephs Fjord. *Bull. Grønlands geol. Unders.* 139, 56 pp.

Davies, G. R., Nassichuck, W. W. & Beauchamp, B. 1989: Upper Carboniferous 'Waulsortian' reefs, Canadian Arctic Archipelago. *In* Geldsetzer, H. H. J., James, N. P. & Tebbutt, G. E. (ed.), Reefs – Canada and adjacent areas. *Mem. Can. Soc. Petrol. Geol.* **13**, 658–666.

Dickson, J. A. D. 1965: A modified staining technique for carbonates in thin section. *Nature* **205**, 587 only.

Dunham, R. J. 1962: Classification of carbonate rocks according to depositional texture. *In* Ham, W. E. (ed.) Classification of carbonate rocks. *Mem. Amer. Assoc. Petrol. Geol.* **1**, 108–121.

Füchtbauer, H. 1980: Composition and diagenesis of a stromatolitic bryozoan bioherm in the Zechstein 1 (northwestern Germany). *Contr. Sedimentology* **9**, 233–251.

Hansen, K. 1988: Preliminary report of fussion track studies in the Jameson Land basin, East Greenland. *Rapp. Grønlands geol. Unders.* **140**, 85–89.

Harpøth, O., Pedersen, J. L., Schønwandt, H. K. & Thomassen, B. 1986: The mineral occurrences of central East Greenland. *Meddr Grønland Geosci.* **17**, 139 pp.

Hollingworth, N. T. J. & Tucker, M.E. 1986: The Upper Permian (Zechstein) Tunstall Reef of North East England: palaeoecology and early diagenesis. *In* Peryt, T. M. (ed.) *The Zechstein facies in Europe. Lecture notes in earth science* **10**, 23–50, Berlin: Springer Verlag.

Hurst, J. M., Scholle, P. A. & Stemmerik, L. 1989: Submarine cemented bryozoan mounds, Upper Permian, Devondal, East Greenland. *In* Geldsetzer, H. H. J., James, J. P. & Tebbutt, G. E. (ed.), Reefs – Canada and adjacent area. *Mem. Can. Soc. Petrol. Geol.* **13**, 672–676.

Marcussen, C., Christiansen, F. G., Larsen, P.-H., Olsen, H., Piasecki, S., Stemmerik, L., Bojesen-Koefoed, J. Jepsen, H. F. & Nøhr-Hansen, H. 1987: Studies of the onshore hydrocarbon potential in East Greenland 1986–1987: field work from 72° to 74°N. *Rapp. Grønlands geol. Unders.* **135**, 72–81.

Maync, W. 1961: The Permian of Greenland. *In* Raasch, G. O. (ed.) *Geology of the Arctic* **1**, 214–223, Toronto University Press.

Scholle, P. A., Stemmerik, L. & Harpøth, P. 1990: Origin of a major karst-associated celestite mineralization in Karstryggen, central East Greenland. *J. Sed. Petrol.* **60**, 397–410.

Scholle, P. A., Stemmerik, L. & Ulmer, D. S. in press: Diagenetic history and reservoir potential of Upper Permian carbonate buildups, Wegener Halvø area, Jameson Land basin, East Greenland. *Bull. Amer. Assoc. Petrol. Geol.*

Smith, D. B. 1981: The Magnesian Limestone (Upper Permian) reef complex of northeastern England. *In* Toomey, D. F. (ed.) European fossil reef models. *Spec. Publ. Soc. Econ. Pal. Mineral.* **30**, 161–186.

Springer, N. 1989: Conventional core analysis for GGU. Samples from East Greenland. *Geol. Survey Denmark Internal Report* **59**, 14 pp.

Stemmerik, L. 1989: Crinoid-bryozoan reef mound, Upper Carboniferous Amdrup Land, eastern North Greenland. *In* Geldsetzer, H. H. J., James N. P. & Tebbutt, G. E. (ed.), Reefs – Canada and adjacent area. *Mem. Can. Soc. Petrol. Geol.* **13**, 690–694.

Stemmerik, L., Scholle, P. A., Thomas, E., Amandolia, M., Henk, F. H. & Uncini, G. 1989: Facies mapping and reservoir evaluation of the Upper Permian Wegener Halvø Formation in Wegener Halvø, East Greenland. *Rapp Grønlands geol. Unders.* **145**, 84–87.

Stemmerik, L., Scholle, P. A., Henk, F. H., Di Liegro, G. & Ulmer, D. S. in press: Sedimentology and diagenesis of the

Upper Permian Wegener Halvø Formation carbonates along the margins of the Jameson Land basin, East Greenland. *In* Vorren, T. O. *et al.* (ed.) Arctic geology and petroleum potential. Elsevier.

Surlyk, F., Callomon, J. H., Bromley, R. G. & Birkelund, T. 1973: Stratigraphy of the Jurassic – Lower Cretaceous sediments of Jameson Land and Scoresby Land, East Greenland. *Bull. Grønlands geol. Unders.* **105,** 76 pp.

Surlyk, F., Hurst, J. M. Piasecki, S., Rolle, F., Scholle, P. A., Stemmerik, L. & Thomsen, E. 1986: The Permian of the Western Margin of the Greenland Sea – A future exploration target. *In* Halbouty, M. T. (ed.) Future petroleum provinces of the world. *Mem. Amer. Assoc. Petrol. Geol.* **40,** 629–659.

Tucker, M. E. & Hollingworth, N. T. J. 1986: The Upper Permian reef complex (EZ1) of north east England: Diagenesis in a marine to evaporitic setting. *In* Schroeder, J. H. & Purser, B. H. (ed.) *Reef diagenesis,* 270–290. Berlin: Springer Verlag.

Plate 1

Fig. 1. Partly dissolved botryoid of square-tipped calcite crystal. Note concentric laminae within the cement which was defined by pelloids and encrusting foraminifers during early growth. Also note rim of hydrocarbons between early and late (blue) cement. GGU 303129–49.

Fig. 2. Early marine cement with algal lamination. Vugs formed as the result of fresh water leaching are now filled by late cement (blue). GGU 303129–45.

Fig. 3. Brecciated marine cementstone where crusts of early marine cement have been fractured and are encased in a new generation early cement. Note pervasive early cementation in solution-enlarged fractures and colour zonation of late cement. GGU 303130–110.

Fig. 4. Early fracture partly filled by early cement. Note that part of the post-fracture-cement is dissolved subsequently indicating several stages of freshwater flushing. Also note apparent late fractures with no early cement. GGU 303130–127.

Plate 2

Fig. 1. Bryozoan-foraminifer boundstone with hydrocarbon filled moulds after tubular foraminifers. GGU 303130–44.

Fig. 2. Bivalve-oncoid grainstone with hydrocarbon filled moulds mainly after tubular foraminifers. GGU 303129–60.

Fig. 3. Violet-stained late cement and associated galena (g) in a fracture. Note that hydrocarbon residue pre-dates late cement (arrow). GGU 303129–58.

Fig. 4. Bryozoan-foraminifer packstone with fluorite (f) in a solution enlarged vug. Note hydrocarbons in stylolite. GGU 303129–21.

Plate 3

Fig. 1. Vug filled with hydrocarbon residue (arrow). GGU 303129–59.

Fig. 2. Baryte (b) and fluorite (f) crystals associated with coarsely crystalline, late cement. Cross polarised light. GGU 303130–5.

Fig. 3. Rim of hydrocarbon residue between early cement (right) and violet-stained late cement (left). GGU 303129–60.

Fig. 4. Calcite cement with scalenohedral termination lining a fracture. Dark area to the left is coarsely crystalline, late cement. Cross-polarised light. GGU 303130–134.

Fig. 5. Rim of hydrocarbon residue between early cement (top) and blue-stained late cement. GGU 303117–94.

Fig. 6. Partly disolved fibrous cement where vugs are filled by late, more coarsly crystalline cement (l). Cross polarised light. GGU 303129–45.
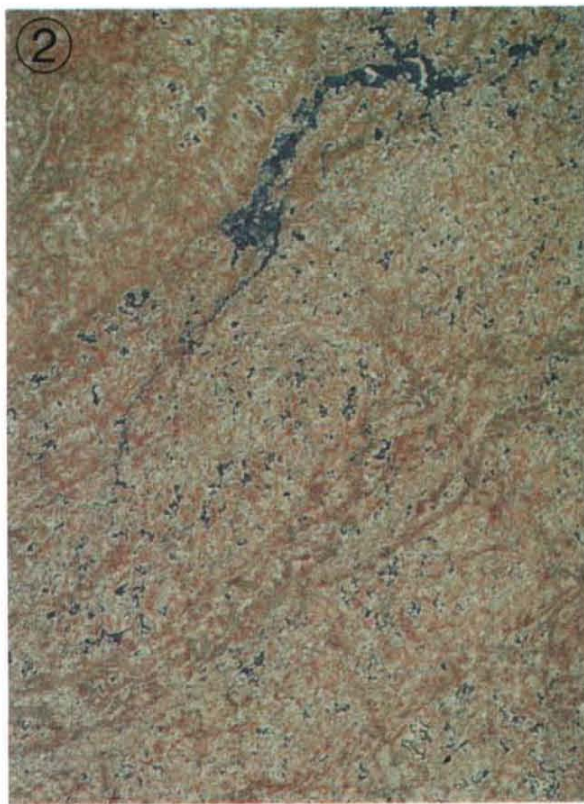
Plate 1

Plate 2

5 mm

Plate 3